Mon. Not. R. Astron. Soc. **367,** 400–406 (2006) doi:10.1111/j.1365-2966.2005.09960.x

Improved HCN/HNC linelist, model atmospheres and synthetic spectra for WZ Cas

G. J. Harris,[1⋆] J. Tennyson,[1] B. M. Kaminsky,[2] Ya. V. Pavlenko[2,3] and H. R. A. Jones[3]

[1]*Department of Physics and Astronomy, University College London, London WC1E 6BT*
[2]*Main Astronomical Observatory, National Academy of Sciences, Zabolotnoho 27, Kyiv-127 03680, Ukraine*
[3]*Centre for Astrophysics Research, University of Hertfordshire, Hatfield AL10 9AB*

Accepted 2005 December 1. Received 2005 November 30; in original form 2005 September 23

ABSTRACT

We build an accurate data base of 5200 HCN and HNC rotation–vibration energy levels, determined from existing laboratory data. 20 000 energy levels in the Harris et al. linelist are assigned approximate quantum numbers. These assignments, lab-determined energy levels and Harris et al. energy levels are incorporated in to a new energy level list. A new linelist is presented, in which frequencies are computed using the lab-determined energy levels where available, and the *ab initio* energy levels otherwise.

The new linelist is then used to compute new model atmospheres and synthetic spectra for the carbon star WZ Cas. This results in better fit to the spectrum of WZ Cas in which the absorption feature at 3.56 μm is reproduced to a higher degree of accuracy than has previously been possible. We improve the reproduction of HCN absorption features by reducing the abundance of Si to [Si/H] $= -0.5$ dex, however, the strengths of the $\Delta v = 2$ CS band heads are overpredicted.

Key words: molecular data – stars: AGB – stars: atmospheres – stars: carbon – infrared: stars.

1 INTRODUCTION

Cool asymptotic giant branch (AGB) carbon stars often show a strong absorption feature at 3 μm. This feature was discovered (Johnson & Mendez 1970) and later identified as the C–H stretch mode of HCN and/or C_2H_2 (Ëay & Ridgeway 1976; Ridgeway, Carbon & Hall 1978). Subsequent to the discovery of HCN in observed carbon star spectra, it was found that the line opacity of HCN has a strong effect upon the structure of model atmospheres (Eriksson et al. 1984; Jørgensen et al. 1985). Harris, Polyansky & Tennyson (2002b), referred to as HPT, have made publicly available an extensive and accurate *ab initio* HCN and HNC linelist. This linelist has been used to compute model atmospheres and synthetic spectra that reproduce the HCN features in the observed spectra of the carbon stars TX Psc and WZ Cas and has also allowed the identification of HNC absorption at 2.9 μm (Harris et al. 2003). However, the HPT linelist has inherent inaccuracies which result in the line frequencies deviating from laboratory measurements by 3 cm^{-1} or more. This error is sufficiently large to be noticeable at the resolving power of the ISO short wavelength spectrometer. In particular, Harris et al. (2003) fail to accurately reproduce the observed HCN Q-branch absorption feature at 3.56–3.62 μm.

In this work, we assign approximate quantum numbers to 20 000 of the HPT *ab initio* energy levels. The quality of the HPT linelist is improved by substituting energy levels derived from laboratory measurements of line frequencies, for *ab initio* energy levels. This improves the frequencies of the lines for which experimental data are available, to spectroscopic precision (0.1 cm^{-1}), and allows the calculation of more accurate C-star synthetic spectra. These new synthetic spectra significantly improve the reproduction of the HCN Q-branch absorption feature at 3.56–3.62 μm.

⋆E-mail: greg@theory.phys.ucl.ac.uk

2 ENERGY LEVEL ASSIGNMENTS

The linelist of Harris et al. (2002b) is calculated using the only exact quantum numbers for a hetronuclear triatomic, angular momentum (J) and parity. Conversely laboratory data are generally presented in terms of the approximate vibrational quantum numbers C–H stretch (v_1), bend (v_2), C–N stretch (v_3), vibrational angular momentum (l) and isomer (HCN or HNC). Where l can take values of 0 or 1, if v_2 is even or odd, and up to $l \leqslant v_2$ and $l \leqslant J$, in steps of 2. Thus for a $v_2 = 4$ with $J \geqslant 4$, l can take values of 0, 2, 4, but for $J = 2$ or $J = 3$, l can only take values of 0 or 2. Fig. 1 is a schematic showing the distribution of even parity energy levels as a function of J and energy. New energy levels appear with each higher J, these are the $l = J$ states. In order to match the lab-determined energy levels with their corresponding *ab initio* energy levels, it is necessary to assign the approximate quantum numbers to the *ab initio* energy level list.

By comparison with the assignments of Bowman et al. (1993) the non-rotating ($J = 0$) vibrational states were assigned by hand up

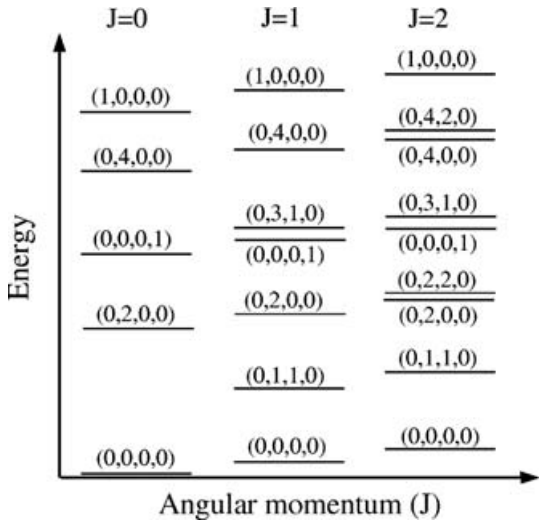

Figure 1. A schematic showing the distribution of even parity HCN energy levels as a function of angular momentum (J) and energy. States are labelled (v_1, v_2, l, v_3).

to 10 000 cm^{-1} above the zero-point energy. We then least-squares fitted the vibrational expansion,

$$E(v,l)+E_0=\sum_{i=1}^{3}\omega_i(v_i+d_i/2)+\sum_{i=1}^{3}\sum_{j=1}^{3}x_{ij}(v_i+d_i/2)(v_j+d_j/2)+x_l l^2, \quad (1)$$

to the assigned energy levels. Where E_0 is the zero-point energy, ω_i are the harmonic constants, x_{ij} are the anharmonic constants, the degeneracies are $d_1=d_3=1$ and $d_2=2$. HCN and HNC states were fitted separately. For $J=0$, x_l is zero. As found by Maki & Mellau (2001) these vibrational expansions give poor fits to both HCN and HNC; however, the fits were useful in identifying and correcting misassigned states.

A somewhat different assignment strategy is required, for $J>0$, as the $l>0$ states do not occur for $J=0$. The distribution of energy levels in a vibrational band of HCN can be approximated by using the rotational expansion for a linear triatomic molecule:

$$E(v,J)=E(v)+B_v[J(J+1)+l^2]-D_v[J(J+1)+l^2]^2+H_v[J(J+1))+l^2]^3+\cdots, \quad (2)$$

where $E(v)$ is the vibrational energy of the band, B_v is the rotational constant, D_v is the centrifugal distortion constant and H_v is a higher-order constant. To estimate the $J=1, l=0$ energy levels, we used the ground vibrational state values of the rotational constant (B_v) of 1.478 221 and 1.512 112 cm^{-1} for HCN and HNC, respectively, and the first two terms of equation (2). By comparing these estimated energy levels with the *ab initio* levels the $J=1, l=0$ states were assigned. The remaining states were those with $l=1$, the lowest energy of these states is the (0, 1^1,0), bending fundamental which was assigned. The vibrational expansion equation (1) was used to fit the newly assigned $J=1, l=0$ and (0, 1^1,0) states and thus estimate values for the higher $J=1, l=1$ states. Again, by comparison of the estimated values with the *ab initio* values, the $J=1, l=1$ states were assigned.

Higher J states were assigned in the same way, the rotational expansion was fit to the previously assigned data for each band, the $l<J$ states assigned by comparison. These assigned $l<J$ states were fitted with the vibrational expansion, allowing the assignment of the $l=J$ states. This process was carried out on a J by J basis until energy levels up to $J=60$ had been assigned. In total, we assigned approximate quantum numbers to around 20 000 energy levels, for HCN this is up to 3 quanta of H–C stretch, 13 quanta of bend and 4 quanta of C–N stretch.

The distribution of the line strengths of a given band can be approximated by Hönl–London factors. By fitting the line transition dipoles of each band using Hönl–London factors is possible to identify lines which have an intensity which is inconsistent with that of the band as a whole. In this way we cross-checked the consistency of our assignments, using line intensities, and corrected our assignments where necessary. However, there are states in the linelist of HPT which are close enough in both energy and quantum numbers for intensity stealing to break the distribution of intensities in a band; see Harris, Polyansky & Tennyson (2002a). For these states the assignment of approximate quantum numbers, based on energy and/or transition dipole, is difficult and arguably meaningless; such states are left unassigned.

3 ENERGY LEVELS DETERMINED FROM LABORATORY DATA

HCN and HNC have been studied in detail in the laboratory (Smith et al. 1989; Northrup, Bethardy & Macdonald 1997; Lecoutre et al. 2000; Maki et al. 2000; Maki & Mellau 2001). HCN has been studied up to a maximum of 6 quanta in the bending and H–C stretch modes and 4 quanta in the C–N stretch mode. Because of its nature, HNC is more difficult to produce in the lab thus data are less extensive than for HCN, up to 2 quanta of bend, 4 quanta of H–N stretch and 2 quanta on C–N stretch. This laboratory data are presented in varying formats, from line frequencies to fits of polynomial expansions in angular momentum, such as equation (2). Using the electronic data base of laboratory line frequencies from Northrup et al. (1997); Maki et al. (2000); Maki & Mellau (2001), we have computed and compiled a list of HCN/HNC energy levels relative to the zero-point energy of HCN. For any given band some or many line frequencies remain unmeasured, there are, therefore, missing energy levels in many of the vibrational states. These missing energy levels can be interpolated by means of the rotational expansion for a linear molecule equation (2). For a given vibrational excitation, l, and parity, we least-squares fit equation (2) to our lab-determined energy levels to obtain $E(v)$, B_v, D_v and H_v. These constants are then used to interpolate any missing energy levels.

In the high temperatures of a stellar atmosphere, the HCN molecule can be excited to a very high angular momentum. HPT found that at 3000 K states up to $J=60$ contribute up to 93 per cent of the rotationally converged partition function. The maximum rotational excitation in our lab-determined linelist is $J=55$, the minimum is $J=20$, to match HPT we must extrapolate to $J=60$. As the rotational expansion (equation 2) is divergent, it is not physically realistic and is, therefore, unsuitable for extrapolation to high J. In order to extrapolate to $J=60$, we correct the *ab initio* energy levels of HPT by adding a constant for a given vibrational state, l, and parity. This constant is given by $C=E_{\rm lab}(J_{\rm max})-E_{\rm ai}(J_{\rm max})$, where $E_{\rm lab}(J_{\rm max})$ is the energy of the state in the laboratory energy

Table 1. A sample from the lab/empirical energy level list, which is available in full, in electronic form, from either the CDS archive (http://cdsweb.u-strasbg.fr/cgi-bin/qcat?/MNRAS/) or from our website (http://www.tampa.phys.ucl.ac.uk/ftp/astrodata).

Index	J	P	n	$E_{\rm ai}$ (cm^{-1})	iso	v_1	v_2	l	v_3	$E_{\rm lab}$ (cm^{-1})	Error (cm^{-1})	Label
1772	3	1	22	4704.012 753	0	1	2	0	0	4702.019 193	3.00E-04	e
1773	3	1	23	4719.910 847	0	1	2	2	0	4716.909 245	4.58E-04	e
1774	3	1	24	4880.708 077	0	0	7	1	0			
1775	3	1	25	4909.459 579	0	0	1	1	2	4895.763 446	2.00E-04	e
1776	3	1	26	4909.583 711	0	0	4	0	1	4906.162 828	2.04E-01	c
1777	3	1	27	4910.798 531	0	0	7	3	0			
1778	3	1	28	4925.183 847	0	0	4	2	1	4920.596 764	8.51E-02	c
1779	3	1	29	5203.782 210	1	0	0	0	0	5203.779 963	5.00E-07	e

level list with the highest angular momentum ($J_{\rm max}$), and $E_{\rm ai}$ ($J_{\rm max}$) is the energy of the *ab initio* energy level with $J = J_{\rm max}$.

The interpolated and extrapolated list of lab-determined energy levels is referred to as the lab/empirical energy level list. It contains 5200 HCN/HNC energy levels up to a maximum of 6 quanta in bend, 3 quanta of H–C stretch and 3 quanta of C–N stretch and to a maximum angular momentum (J) of 60. We have incorporated the lab/empirical energy levels, the 20 000 assignments in to the original *ab initio* energy level list of HPT. A sample of this new energy level list is given in Table 1, the full list can be downloaded from our website (http://www.tampa.phys.ucl.ac.uk/ftp/astrodata) or the CDS archive (http://cdsweb.u-strasbg.fr/cgi-bin/qcat?/MNRAS/).

The column labelled index in Table 1 is the index number given to the energy level by HPT, J and P are the exact quantum numbers of angular momentum and parity, n is the number of the energy level in the J–P symmetry block, $E_{\rm ai}$ is the value of the *ab initio* energy level, iso labels the state as either HCN (iso = 0) or HNC (iso = 1), v_1, v_2, l and v_3 are the approximate quantum numbers, $E_{\rm lab}$ is the lab/empirical energy, label is a single character label which is either 'e' for a lab-determined energy level, 'c' for an interpolated energy level or 't' for a corrected *ab initio* energy level. The error on the energy level takes three forms, for a lab-determined energy level this is the compound error of the line frequency measurements used to derive the energy level. For an interpolated energy level, this is the standard deviation on the fit of equation (2). For a corrected *ab initio* energy level, the error is the difference between the energy predicted by the fit of equation (2), to lab and empirical energy levels, and the corrected '*ab initio*' energy. The errors of the lab-determined energy levels are typically of the order of 10^{-4} cm^{-1}, the errors on the interpolated energy levels are typically of the order of 10^{-2} cm^{-1}, and of the order of 1 cm^{-1} on the corrected *ab initio* energy levels.

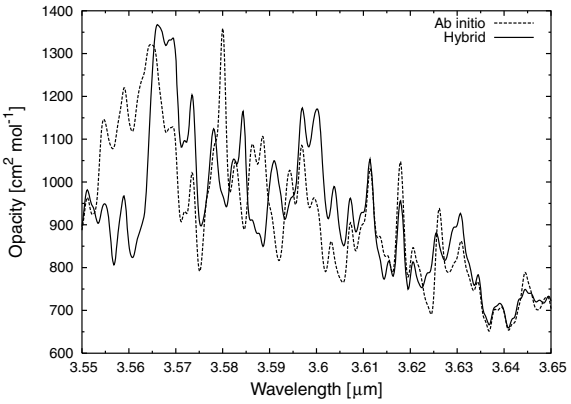

Figure 2. The opacity function of HCN/HNC at 2800 K, the lines have been broadened by a Gaussian with half width at half maximum of 0.003 μm.

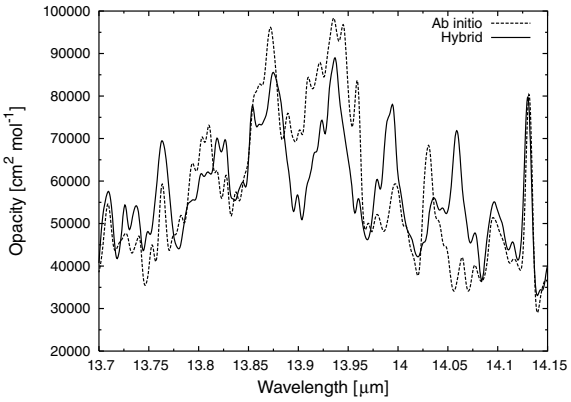

Figure 3. The opacity function of HCN/HNC at 2800 K, the lines have been broadened by a Gaussian with half width at half maximum of 0.003 μm.

4 THE NEW LINELIST

The lab/empirical and *ab initio* energy levels, together with the Einstein A coefficients from the HPT linelist, allow the generation of a new hybrid linelist. For the majority of lines, the line frequencies are computed from the original *ab initio* energy levels. However, if lab/empirical energy levels have been determined for both the upper and lower states, we can use the lab/empirical energy levels to compute a more accurate line frequency. The resulting linelist significantly improves the accuracy of the most intense transitions between the low-lying energy levels. This improvement in the linelist is evident in Figs 2 and 3, which show opacity functions calculated with both the *ab initio* and hybrid linelists. The predominant features in these opacity functions are the Q branches of the ($\Delta v_2 = 1 + \Delta v_3 = 1$) and ($\Delta v_2 = 1$) bands, respectively. As the Q branches have a large concentration of lines over a small frequency range, it is with these Q branches that the improvements within the synthetic spectrum are most evident.

To maintain accuracy and consistency when computing a line frequency, it is important to use either *ab initio* or lab/empirical energy levels for both the upper and lower states. The error on a given *ab initio* energy level in general increases with an increasing value of a quantum number. For example, the deviation of the (0,0^0,1) $J = 0$ *ab initio* energy level from laboratory determination is +3.7 cm^{-1}, for the (0,0^0,2) and (0,0^0,3) states the deviation is +8.4 and +13.8 cm^{-1}.

Table 2. A sample from the hybrid line list, the strongest 34.4 million of which are available, in electronic form, from either the CDS archive http://cdsweb.u-strasbg.fr/cgi-bin/qcat?/MNRAS/ or from our website http://www.tampa.phys.ucl.ac.uk/ftp/astrodata.

ν (cm^{-1})	E'' (cm^{-1})	J''	p''	n''	J'	p'	n'	$A_{\rm if}$ (s^{-1})	Index$''$	Index$'$	iso$''$	v''_1	v''_2	l''	v''_3	iso$'$	v'_1	v'_2	l'	v'_3	label
2.956 432	0.000 000	0	1	1	1	1	1	2.263E-05	1	99 631	0	0	0	0	0	0	0	0	0	0	lb
2.957 251	12 055.741 477	0	1	92	1	1	171	1.794E-05	92	99 801	−2	−2	−2	−2	−2	−2	−2	−2	−2	−2	ai
2.957 637	4888.417 867	0	1	10	1	1	17	2.015E-05	10	99 647	0	0	4	0	1	0	0	4	0	1	lb
2.957 871	12 150.505 903	44	0	161	44	1	206	6.785E-07	141 511	140 356	1	0	8	6	0	1	0	0	0	2	ai
2.958 350	11 744.486 505	0	1	87	1	1	162	2.200E-05	87	99 792	−2	−2	−2	−2	−2	−2	−2	−2	−2	−2	ai
2.958 460	8691.662 400	0	1	37	1	1	68	1.923E-05	37	99 698	0	1	8	0	0	0	1	8	0	0	ai

Thus when calculating frequencies between excited states using the *ab initio* energy levels there is, more often than not, a partial cancellation of error. This is not the case if a combination of lab/empirical and *ab initio* energy levels are used to calculate frequency, which results in a larger error on frequency.

To reduce the required storage space and increase the speed of computations using our linelist, we have truncated the hybrid linelist at a minimum intensity of 3×10^{-28} cm molecule^{-1} at 3000 K. This results in a linelist of 34.4 million lines less than 10 per cent of the 393 million lines in the original linelist. These 34.4 million lines account for more than 99.99 per cent of the opacity of the full linelist at a temperature of 3000 K. A sample of the linelist is given in Table 2, here ν is frequency, E'' is lower-state energy, $A_{\rm if}$ is the Einstein A coefficient, J'' and J' are lower-state and upper-state angular momentum quantum numbers, p is parity where 1 is even and 0 odd, n is the number of the level in the J-parity block, index is the unique label of the energy level, iso labels a HCN state if 0 or a HNC state if 1, v_1, v_2, l, v_3 are the approximate quantum numbers. Where the approximate quantum numbers have not been assigned a value of −2 is given. The full version of the linelist is available from either the CDS archive http://cdsweb.u-strasbg.fr/cgi-bin/qcat?/MNRAS/ or from our website http://www.tampa.phys.ucl.ac.uk/ftp/astrodata. The file size is 3.6-Gb uncompressed and 821-Mb compressed using bzip2. The linelist is sorted in ascending frequency order.

The untruncated linelist can be obtained by downloading the original HPT Einstein A coefficients, the new assigned energy level list and running the supplied FORTRAN utility program DPSORT-v2.0.f90. The Einstein A coefficient file from HPT is sorted using *ab initio* frequencies, if lab-determined frequencies are used the linelist will no longer be in full frequency order.

The integrated absorption intensity of the lines can be computed from the Einstein A coefficient using

$$I = \frac{C(2J'+1)}{Q_{\rm vr}\nu^2} \exp\left(\frac{-E''}{kT}\right)\left[1-\exp\left(\frac{-\nu}{kT}\right)\right] A_{\rm if}, \quad (3)$$

where I is integrated intensity, $Q_{\rm vr}$ is the ro-vibrational partition function, J' is the upper state rotational quantum number, ν is the transition wavenumber, E'' is the lower-state energy, C is a constant and $A_{\rm if}$ is the Einstein A coefficient. To return I in cm per molecule, with $A_{\rm if}$ in s^{-1} and ν in cm^{-1}, C has the value of $(8\pi c)^{-1} = 1.3271 \times 10^{-12}$ s cm^{-1}. The authors recommend the use of the Barber, Harris & Tennyson (2002) rotationally converged HCN/HNC partition function. Dimensionless oscillator strengths are often used by those involved in the modelling of stellar atmospheres. Weighted oscillator strengths (gf) can be computed from the Einstein A coefficients using

$$gf = \frac{K(2J'+1)}{\nu^2} A_{\rm if}, \quad (4)$$

where K is a constant which for cgs units (ν in cm^{-1} and $A_{\rm if}$ in s^{-1}) has the value

$$K = \frac{m_{\rm e}c}{8\pi^2 e^2} = 1.499197\ {\rm s\,cm^{-2}}, \quad (5)$$

and for SI units (ν in m^{-1} and $A_{\rm if}$ in s^{-1}) the value

$$K = \frac{m_{\rm e}\epsilon_0 c}{2\pi e^2} = 14991.97\ {\rm s\,m^{-2}}. \quad (6)$$

5 COMPUTATION OF MODEL ATMOSPHERES AND SYNTHETIC SPECTRA

We computed the model atmospheres of C-giants with the SAM12 program (Pavlenko 2003a, b) which is a modification of ATLAS12 (Kurucz 1996). SAM12 is a plane parallel code which makes use of the local thermodynamic equilibrium (LTE) approximation, hydrostatic equilibrium and the conservation of flux (there are no sources or sinks of energy within the atmosphere). The photospheres of C-giants lie on the upper boundary of their convective envelopes, thus convection plays an important role in these atmospheres. We use the mixing length theory of 1D convection modified by Kurucz (1996) in ATLAS12, and adopt a value of the mixing length parameter of $l/H = 1.6$.

SAM12 uses the standard set of continuum opacities included in ATLAS12, with the addition of continuous opacities from C^- (Myerscough & McDowell 1966), H_2^- (Doyle 1968) and bound-free absorption of C, N, O from TOPBASE (Seaton, Zeipen & Tully 1992) with cross-sections from Pavlenko & Zhukovska (2003). These bound-free opacity tables have been made available on the web.[1] Atomic and molecular lines opacities were accounted for by using the opacity sampling approach (Sneden, Johnson & Krupp 1976). The data for these lines were obtained from several sources. HCN/HNC lines taken from this work, atomic lines from the Vienna Atomic Line Database (VALD) data base (Kupka et al. 1999), CN, C_2, SiH, MgH, CH from CD-ROM 18 of Kurucz (1992), CO from Goorvitch (1994), and CS from Chandra et al. (1995). The following molecular electronic bands were accounted for: CaO($C^1\Sigma$–$X^1\Sigma$), CS($A^1\Sigma$–$X^1\Sigma$), SO($A^3\Pi$–$X^3\Sigma$), SiO($E^1\Sigma$–$X^1\Sigma$), SiO($A^1\Pi$–$X^1\Sigma^+$, NO($C^2\ \Pi_r$–$X^2\Pi_r$), NO($B^2\Pi_r$–$X^2\Pi_r$), NO($A^2\Sigma^+$–$X_2\Pi_r$), MgO($B^1\Sigma^+$–$X^1\Sigma^+$), AlO($C^2\Pi$–$X^2\Sigma$), AlO($B^2\Sigma^+$–$X^2\Sigma^+$), in the framework of the just-overlapping line approach (JOLA). For WZ Cas these electronic bands are only week sources of opacity. For all cases we adopted the carbon isotopic ratio $^{12}C/^{13}C$ of 5. The shape of every line was determined using the Voigt function $H(a, v)$. Damping constants were taken from line data bases or computed using Unsold's approach (Unsold 1955). In model atmosphere computations, we adopt a microturbulent velocity, $V_{\rm t}$, of 3.5 km s^{-1}.

[1] http://www.mao.kiev.ua/staff/yp/Results/CNO_bf.tar.gz

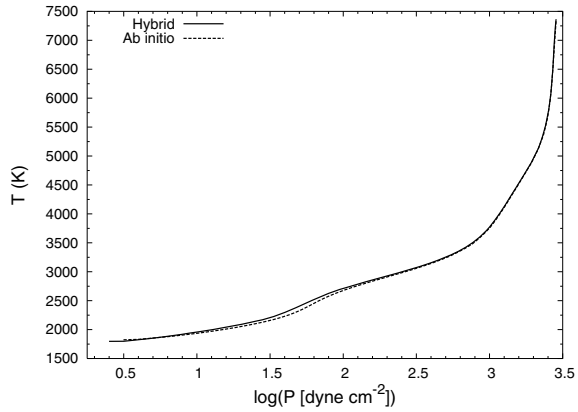

Figure 4. Temperature–pressure curves of model atmospheres of $T_{\rm eff}$ = 2800 K, log $(N_C/N_O) = -0.003$, log $(g) = 0.0$, computed with the *ab initio* and hybrid linelists.

Model atmospheres were computed using the 'best-fit' effective temperature and C/O ratio, found in our earlier work (Harris et al. 2003), $T_{\rm eff}$ = 2800 K, log $(N_C/N_O) = -0.003$, log $(g) = 0.0$. Fig. 4 shows the pressure–temperature curves of model atmospheres computed with the *ab initio* linelist and hybrid linelist. There is little difference between the atmospheres at depth, but at lower optical depths the model atmosphere computed with the hybrid linelist is slightly hotter at a given pressure.

Synthetic spectra were calculated with the WITA6 program (Pavlenko 2000), using the same approximations and opacities as SAM12, but with a considerably finer grid of wavelength points ($\Delta\lambda = 0.01$–0.02 Å). We have also computed synthetic spectra with reduced S and Si abundances of [Si/H] = 0 and -0.5 dex to attempt to better-fit HCN absorption and reduce the strength of CS absorption; see Section 6.1.

6 COMPARISON OF SYNTHETIC SPECTRA WITH OBSERVED STELLAR SPECTRA

The observations of WZ Cas used in this study were taken as part of the Japanese guaranteed observing time (REDSTAR1, PI T. Tsuji, e.g. Aoki, Tsuji & Ohnaka 1998). The data and data reduction used in this work are discussed in detail in our earlier paper (Harris et al. 2003).

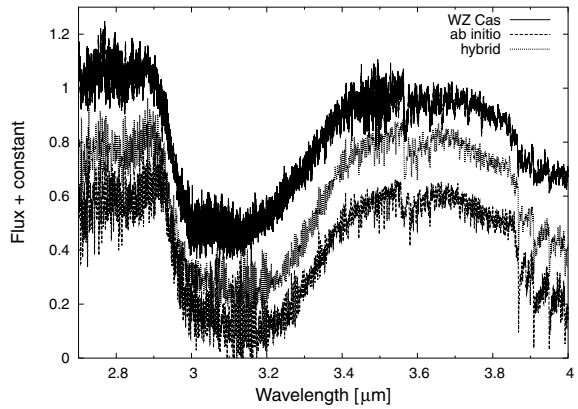

Figure 5. Synthetic and observed spectra of WZ Cas. The synthetic spectra have been convolved with by a Gaussian with half width at half maximum of 0.003 μm. The synthetic spectra have constants of 0.2 and 0.4 subtracted from the flux.

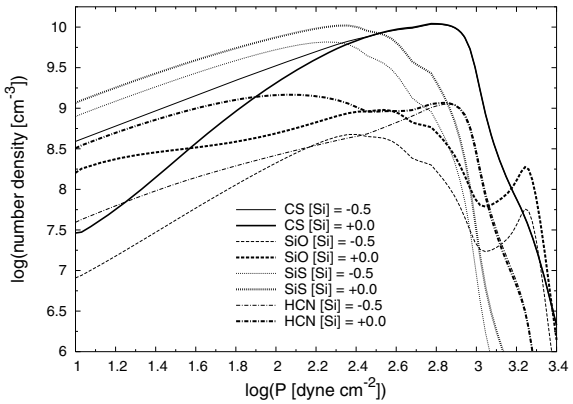

Figure 6. Number densities of HCN, CS, SiO and SiS as a function of pressure in the model atmospheres with [Si/H] = 0 and -0.5 dex.

Synthetic and observed spectra of WZ Cas between 2.7 and 4.0 μm are shown in Fig. 5. At this resolution there is little difference between the synthetic spectra calculated with the *ab initio* and hybrid linelist. A synthetic spectrum computed with solar abundances results in HCN absorption that is stronger than in the observed spectrum WZ Cas. We find that [Si/H] $= -0.5$ provides the best fit of HCN features. The reason for this is that in carbon rich atmospheres silicon and sulphur have a strong secondary affect on chemical equilibrium, after carbon and oxygen (Tsuji 1973). Indeed, SiS is analogous to CO and is a very stable molecule, thus atmospheres with a high ratio of Si to S are silicon rich and those with a low ratio are silicon poor. Fig. 6 shows the number densities of CS, SiO, SiS and HCN, as a function of pressure in our model atmospheres computed with [Si/H] = 0 and -0.5 dex. As the abundance of silicon is reduced from [Si/H] = 0 to -0.5 dex, there is less SiS and SiO, freeing S and O to form CO and CS, this reduces the abundance of HCN.

At higher resolutions the improvements in line positions in the hybrid linelist become more obvious. Figs 7 and 8 show the synthetic spectra calculated with the *ab initio* and hybrid linelists, and the observed spectrum of WZ Cas, between 3.55–3.61 and 3.84–3.895 μm, respectively. The position of the band centres in Fig. 7 is indicated by an arrow and an index number. The corresponding transitions are given in Table 3. There is a clear improvement of

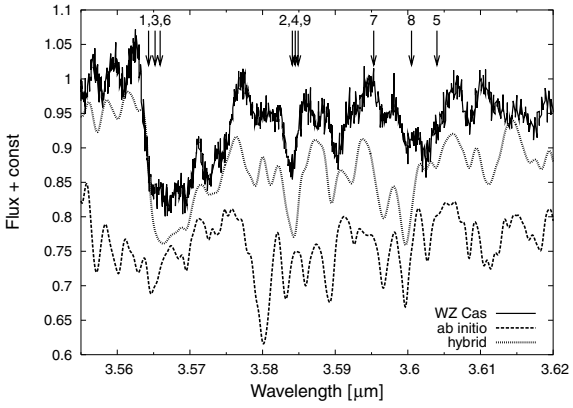

Figure 7. Synthetic and observed spectra of WZ Cas. The synthetic spectra have been convolved with by a Gaussian with half width at half maximum of 0.003 μm. The synthetic spectra have constants of 0.1 and 0.2 subtracted from the flux. HCN band centres are labelled with arrows and an index number for the band which is tabulated in Table 3.

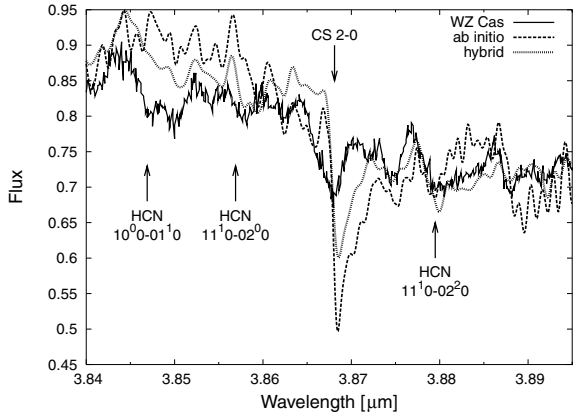

Figure 8. Synthetic and observed spectra of WZ Cas. The synthetic spectra have been convolved with by a Gaussian with half width at half maximum of 0.003 μm.

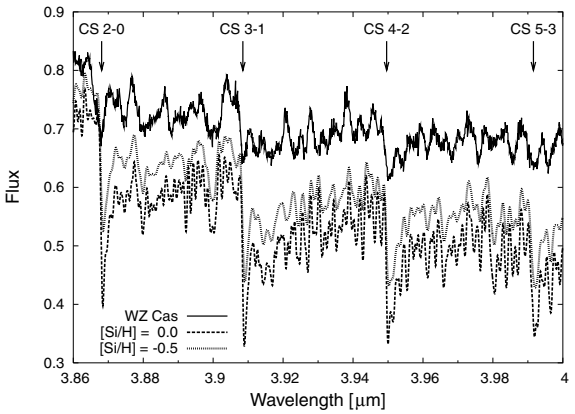

Figure 9. Synthetic and observed spectra of WZ Cas. The synthetic spectra have been calculated with different Si abundances and are convolved with by a Gaussian with half width at half maximum of 0.003 μm. The synthetic spectra have constants of 0.075 and 0.1 subtracted from the flux.

Table 3. Laboratory band centres for bands with $\Delta v_2 = 1$, $\Delta v_3 = 1$.

Index[a]	(v'_1, v'_2, l', v'_3)	$(v''_1, v''_2, l'', v''_3)$	λ_c^b (μm)
1	(0, 1, 1, 1)	(0, 0, 0, 0)	3.5643
2	(0, 2, 0, 1)	(0, 1, 1, 0)	3.5841
3	(0, 2, 2, 1)	(0, 1, 1, 0)	3.5652
4	(0, 3, 1, 1)	(0, 2, 0, 0)	3.5845
5	(0, 3, 1, 1)	(0, 2, 2, 0)	3.6040
6	(0, 3, 3, 1)	(0, 2, 2, 0)	3.5659
7	(0, 1, 1, 2)	(0, 0, 0, 1)	3.5953
8	(0, 4, 0, 1)	(0, 3, 1, 0)	3.6041
9	(0, 4, 2, 1)	(0, 3, 1, 0)	3.5849

[a]This is the index of the band used in Fig. 7.
[b]From the laboratory measurements of Maki et al. (1996).

the fit to observation, across the whole of the 3.55–3.61 μm range. The remaining discrepancies between observed and synthetic spectra over this range are likely to be due either to the spectra of missing chemical species or to transitions between states with $v_2 > 5$, for which laboratory data are unavailable. In Fig. 7, we have labelled the position of the band centres of several HCN bands. Absorption features can be seen close to the band centres, these are due to the Q-branch ($\Delta J = 0$) lines of the band, which are closely spaced and result in strong absorption over a narrow range.

6.1 The CS $\Delta v = 2$ band heads and the abundance of sulphur and silicon

In the 3.84–3.895 μm region shown in Fig. 8, we have identified the Q branches of the three lowest-lying HCN states. The reproduction of the shapes of these HCN absorption features is significantly improved, by the use of the hybrid linelist. However, we overpredict the strength of the CS $v = 0 \rightarrow 2$ band head at about 3.868 μm. Aoki et al. (1998) had the same problem; they suggested that the poor fit was a result of emission by CS from a circumstellar shell. We feel that this is an unlikely scenario. Absorption from both the fundamental and the hot bands is clear in our synthetic spectra, and also appear, all be it more weakly, in the observed spectrum. In contrast, emission from CS at temperature significantly lower than that of the stellar photosphere will be predominantly from the fundamental and the low-lying hot bands. Thus the signature of atmospheric absorption with emission from a cool circumstellar shell would be a weak fundamental band and strong hot bands, this is not seen in the observed spectra.

As an alternative to circumstellar shell emission wetested alternative metal mixes. The problem, however, cannot be solved by reducing the sulphur abundance, because not only are the strength of the CS lines reduced, but chemical equilibrium is altered resulting in a greater abundance of HCN, so that the HCN features from 2.8 to 4 μm were poorly reproduced. Similarly, increasing the abundance of silicon to [Si/H] = 0 dex weakens slightly the CS features, but increases the strength of HCN absorption. The net effect is little improvement in the reproduction of absorption over the 3.8–4 μm region; see Fig. 9, but a worse reproduction of the HCN absorption across the wider spectral range.

We use the CS linelist of Chandra et al. (1995) in our computations, we do not believe that errors in this linelist contribute to the overprediction of the strength of CS features in our synthetic spectra. This CS linelist was calculated by using Dunham coefficients from Winkel et al. (1984), and the dipole moment surface of Botschwina & Sebald (1985). Within the rigid rotor approximation, the rotational $J = 0 \rightarrow 1$ transition dipole is equal to the permanent dipole moment, thus can be used as a rough check for the accuracy of intensity calculations. The $J = 0 \rightarrow 1$ transition dipole computed by Chandra et al. (1995) is 1.889 D, the permanent dipole moment quoted by Botschwina & Sebald (1985) is 1.958 D. The vibrational band transition dipoles given by Botschwina & Sebald (1985) are 0.1580 and 0.00 911 D for the $v = 0 \rightarrow 1$ and $v = 0 \rightarrow 2$ transitions, respectively. The $v = 0 \rightarrow 1$ and $v = 0 \rightarrow 2$ transitions given by Chandra et al. (1995) are 0.1569 and 0.00 788 D. Although there are small differences, this is not large enough to account for the difference between observation and synthetic spectra. A final possibility is that there is an opacity source present in the stellar atmosphere which we have not accounted for in our models. This could be from a species such as C_2H_2, which is known to exist in some C-star atmospheres, but is not included in our calculations, as no C_2H_2 linelist is available. It is possible that increased opacity from such species could affect both the structure of model atmospheres and/or change the synthetic spectra.

7 CONCLUSION

We have assigned approximate quantum numbers to 20 000 of the *ab initio* energy levels found in the HCN/HNC linelist of Harris

et al. (2002b). Existing laboratory measurements of HCN and HNC line frequencies are used to accurately determine 5200 energy levels. Both the energy level assignments and the lab/empirical energy levels have been included along with the *ab initio* energy levels of Harris et al. (2002b) in a new energy level list. A combination of the lab/empirical and *ab initio* energy levels are used in conjunction with the Harris et al. (2002b) Einstein A coefficients to produce an improved linelist. We make the new energy level file which includes assignments, lab-determined energy levels and the resulting improved HCN and HNC linelist publicly available.

The new linelist has been incorporated into our computations of C-rich model stellar atmospheres and synthetic spectra. The new synthetic spectra are a clear improvement over our earlier synthetic spectra (Harris et al. 2003), and show better agreement with the observed spectrum of WZ Cas. The improvement is clearest in the range 3.56–3.62 μm. We further improve the fit to HCN features by reducing the Si abundance to $[\mathrm{Si/H}] = -0.5$ dex, however, the CS absorption feature at 3.8–4.0 μm is still poorly reproduced.

ACKNOWLEDGMENTS

GJH thanks the UK Particle Physics and Astronomy Research Council (PPARC) for post-doctoral funding. The work of YaVP is partially supported by the Leverhume Trust. The manipulation and analysis of the HCN/HNC linelist were carried out on the Enigma computer facility of the HiPerSPACE computing centre at UCL which is partly funded by PPARC.

REFERENCES

Aoki W., Tsuji T., Ohnaka K., 1998, A&A, 340, 222
Barber R. J., Harris G. J., Tennyson J., 2002, J. Chem. Phys., 117, 11239
Botschwina P., Sebald P., 1985, J. Mol. Spectrosc., 110, 1
Bowman J. M., Gazdy B., Bentley J. A., Lee T. J., Dateo C. E., 1993, J. Chem. Phys., 99, 308
Chandra S., Kegel W. H., Le Roy R. J., Hertenstein T., 1995, A&AS, 114, 175
Doyle R. O., 1968, ApJ, 153, 987
Eriksson K., Gustafsson B., Jørgensen U. G., Nordlund Å., 1984, A&A, 132, 37
Ḟay T. D., Ridgeway S. T., 1976, ApJ, 203, 600
Goorvitch D., 1994, ApJS, 95, 535.
Harris G. J., Polyansky O. L., Tennyson J., 2002a, Spectrochim. Acta A, 58, 673
Harris G. J., Polyansky O. L., Tennyson J., 2002b, ApJ, 578, 657 (HPT)
Harris G. J., Pavlenko Ya. V., Jones H. R. A., Tennyson J., 2003, MNRAS, 344, 1107
Johnson H. J., Mendez M. E., 1970, AJ, 75, 785
Jørgensen U. G., Almlöf J., Gustafsson B., Larsson M., Siegbahn P., 1985, J. Chem. Phys., 83, 3034
Kupka F., Piskunov N., Ryabchikova T. A., Stempels H. C., Weiss W. W., 1999, A&AS, 138, 119
Kurucz R. L., 1992, Rev. Mex. Astron. Astrofisica, 23, 45
Kurucz R. L., 1996, in Adelman S. J., Kupka F., Weiss W. W., eds, Proc. Model Atmospheres and Spectrum Synthesis, ASP Conf. Ser. Vol. 108. Astron. Soc. Pac., San Francisco, p. 160
Lecoutre M., Rohart F., Huet T. R., Maki A. G., 2000, J. Mol. Spectrosc., 203, 158
Maki A. G., Mellau G. CH., 2001, J. Mol. Spectrosc., 206, 47
Maki A., Quapp W., Klee S., Mellau G. Ch., Albert S., 1996, J. Mol. Spectrosc., 180, 323
Maki A. G., Mellau G. CH., Klee S., Winnewisser M., Quapp W., 2000, J. Mol. Spectrosc., 202, 67
Myerscough V. P., McDowell M. R. C., 1966, MNRAS, 132, 457
Northrup F. J., Bethardy G. A., Macdonald R. G., 1997, J. Mol. Spectrosc., 186, 349
Pavlenko Ya. V., 2000, Astron. Rep., 44, 219
Pavlenko Y. V., 2003a, in Piskunov N., Weiss W. W., Gray D. F., eds, Proc. IAU Symp. 210, Modelling of Stellar Atmospheres. Astron. Soc. Pac., San Francisco (astro-ph 0209022)
Pavlenko Y. V., 2003b, Astron. Rep., 47, 59
Pavlenko Ya. V., Zhukovska S. V., 2003, Kimemat. Phys. Celest. Bodies, 19, 28
Ridgeway S. T., Carbon D. F., Hall D. N. B., 1978, ApJ, 225, 138
Seaton M. J., Zeipen C. J., Tully J. A., 1992, Rev. Mexic. Astron. Astrophys., 23, 107
Smith A. M., Coy S. L., Klemperer W., Lehmann K. K., 1989, J. Mol. Spectrosc., 134, 124
Sneden C., Johnson H. R., Krupp B. M., 1976, ApJ, 204, 218
Tsuji T., 1973, A&A, 23, 411
Unsold A., 1955, Physik der Sternatmospharen, 2nd edn. Springer-Verlag, Berlin
Winkel R. J., Davis S. P., Pecyner R., Brault J. W., 1984, Can. J. Phys., 62, 1414

This paper has been typeset from a TEX/LATEX file prepared by the author.